Dielectronic recombination of Pd-like gadolinium

B. W. Li* and G. O'Sullivan
School of Physics, University College Dublin, Belfield, Dublin 4, Ireland

Y. B. Fu and C. Z. Dong
Key Laboratory of Atomic and Molecular Physics and Functional Materials of Gansu Province, College of Physics and Electronics Engineering, Northwest Normal University, Lanzhou, 730070, China and
Joint Laboratory of Atomic and Molecular Physics, NWNU and IMP CAS, Lanzhou 730070, China

(Received 30 September 2011; revised manuscript received 16 December 2011; published 30 January 2012)

As research and development of extreme ultraviolet lithography (EUVL) sources at 6.7 nm (which will be based on emission from ionized gadolinium) has already begun, reliable atomic data are required in order to determine the optimum plasma conditions. However, the complexity of the atomic structure means that *ab initio* level-resolved dielectronic recombination (DR) calculations are currently unavailable for the ions of interest. Here we report the first detailed calculation of the DR rate coefficients for the ground state and first excited states of Pd-like gadolinium. Energy levels, radiative transition probabilities, and autoionization rates of Ag-like gadolinium for $[\mathrm{Kr}]4d^9 4fnl$, $[\mathrm{Kr}]4p^5 4d^{10} 4fnl$, $[\mathrm{Kr}]4d^9 5l'nl$, and $[\mathrm{Kr}]4d^9 6l'nl$ ($n \leqslant 18$) complexes were calculated using the flexible atomic code (FAC). It was found that inclusion of $4p^5 4d^{10} 4fnl$ configurations has significant influence on the total DR rate coefficient. The DR rate coefficients obtained here are compared with radiative recombination and three-body recombination coeffcients. The results show that the DR rate coefficient is almost an order of magnitude higher than the coefficients for the other two recombination processes combined at plasma electron temperatures around 110 eV, which suggests that the DR process should be included in theoretical modeling for Pd-like gadolinium in EUVL source plasmas.

DOI: 10.1103/PhysRevA.85.012712 PACS number(s): 34.80.Lx

I. INTRODUCTION

To keep pace with Moore's law, which envisages a doubling of component density on microprocessors every 18 months predicated on a 40% reduction in size, plasmas containing gadolinium have been proposed as sources for next generation lithography. These plasmas emit strongly at wavelengths near 6.7 nm and will succeed the 13.5 nm sources currently being tested on high volume manufacturing tools which are based on emission from ionized tin [1,2]. Use of 6.7 nm radiation will facilitate the production of feature sizes down to a few nanometers thus extending the applicability of Moore's law to semiconductor manufacturing for another ten to 15 years. The choice of tin plasmas for 13.5 nm operation was based on their emitting intense resonance transitions from $4p^6 4d^n$-$4p^5 4d^{n+1} + 4d^{n-1} 4f$ transitions in Sn IX through Sn XIV which lie in the required spectral region [3,4]. In the rare earths, because of the near constancy of the $\langle 4d|4f\rangle$ overlap integral with increasing ionic charge, these transitions overlap in adjacent ion stages to yield a narrow intense unresolved transition array (UTA), consisting of tens of thousands of lines, the peak position of which is sensitive to atomic number and moves to shorter wavelengths as Z increases; in Gd it lies near 6.7 nm [5–7]. As a result, the brightest source at this wavelength has been identified as Gd where conversion efficiencies up to 1.8% of laser energy into emitted extreme ultraviolet (EUV) radiation within a 2% wavelength band centered near 6.7 nm have been measured recently [8]. For a complete understanding of Gd plasma emission, reliable atomic data, such as energy levels, transition probabilities, and dynamic processes rate coefficients are urgently needed. Reliable dielectronic recombination (DR) rate coefficients are crucial for the modeling of the ionization balance in plasmas. Recently, Fu *et al.* have studied the DR rate coefficients in Sn^{10+} [9] and Sn^{12+} [10] ions. They found that the DR process has significant influence on the plasma ionization balance. However, due to the complexity of the calculations, very few *ab initio* level-by-level DR calculations are available for Gd ions. In all reported studies of Gd plasmas, their emission is dominated by Ag- and Pd-like Gd XVIII and Gd XIX lines, i.e., the spectra containing fewest lines resulting from ions with either a closed outermost subshell or a configuration with a single electron outside a closed subshell, where the emission is not spread among many transitions [11,12]. Recently, Safronova *et al.* studied the DR rate coefficients for Pd-like Xe [13] and W [14] which are important for extreme ultraviolet lithography and fusion applications, respectively.

In this paper, we report on the detailed calculation of DR rate coefficients for Pd-like gadolinium. The relativistic flexible atomic code (FAC) [15] was used to calculate the atomic structure, radiative transition probabilities, and autoionization probabilities. In Sec. II we briefly outline the theoretical methods used for the calculation of DR rate coefficients. The DR rate coeffcients obtained are presented and compared with the three-body recombination (TR) and radiative recombination (RR) rate coeffcients in Sec.Sec. III.

II. THEORETICAL METHOD

The DR process can be described as the resonant capture of an incident electron by an ion, followed by radiative decay which competes with autoionization. The first step is the

*libw2007@gmail.com

resonant capture process in which a free electron is captured by an ion while a bound electron is excited. For Pd-like Gd, taking the $4d$ subshell excitation as an example, the capture-excitation process can be schematically written as follows:

$$[\mathrm{Kr}]\,4d^{10} + e \rightarrow [\mathrm{Kr}]\,4d^9 n'l' nl, \quad n'l' = 4f,\ 5l,\ 6l, \qquad (1)$$

It is the inverse process of autoionization, sometimes called dielectronic capture (DC), and the cross sections for DC can be obtained from the autoionization rates through the principle of detailed balance. The DC resonance strength, which corresponds to the integral of the DC cross section over incident electron energies, can be expressed as

$$S_{ij}^{DC} = \frac{\pi^2\hbar^3}{m_e E_{ij}} \frac{g_j}{2g_i} A_{ji}^a, \qquad (2)$$

where g_j and g_i are the statistical weights of the doubly excited autoionization state j and initial state i, respectively, A_{ji}^a is the autoionization rate, and E_{ij} is resonant energy.

The second step in the DR process is autoionizing state decay by emission of either an Auger electron or a photon into a lower state. It can be schematically written as follows:

$$[\mathrm{Kr}]\,4d^9 n'l' nl \rightarrow [\mathrm{Kr}]\,4d^{10} nl + 4d^9 n'l' n''l'' + h\nu, \qquad (3)$$

$$\downarrow$$

$$[\mathrm{Kr}]\,4s^2 4p^6 4d^{10} + e \qquad (4)$$

The first term in Eq. (3) represents the decay from autoionization states to singly excited states, known as resonant stabilizing transitions (RS). The second term represents the decays to doubly excited states which are below the ionization limit, knows as nonresonant stabilizing transitions (NRS). Another possible decay is to those lower states but still lying above the ionization limit and then further decay by either autoionization or spontaneous emission. Therefore, the radiation branching ratio for DR can be writen as

$$B_j^r = \frac{\sum_f A_{jf}^r + \sum_{f'} A_{jf'}^r + \sum_d A_{jd}^r B_d^r}{\sum_{i'} A_{di'}^a + \sum_f A_{jf}^r + \sum_{f'} A_{jf'}^r + \sum_d A_{jd}^r}. \qquad (5)$$

Here A^a and A^r are the autoionization and radiative rates, respectively. f denotes singly excited final states, f' denotes doubly excited final states lying below the ionization limit, d denotes doubly excited final states, and i' corresponds to the final states resulting from the Auger decay (only $4d^{10}$ for the present case). B_d^r is the DR branching ratio of state d and is defined as in Eq. (5). The last term in the denominator of this equation represents decays into autoionizing levels followed by radiative decay cascade (DAC) transition rates. However, as research results show, the DR rates are less affected by DAC for the heavy elements and thus can be neglected for most applications [16]. Disregarding DAC then leads to the following approximation for the DR branching ratio [16]:

$$B_j^r = \frac{\sum_f A_{jf}^r + \sum_{f'} A_{jf'}^r}{\sum_{i'} A_{di'}^a + \sum_f A_{jf}^r + \sum_{f'} A_{jf'}^r}. \qquad (6)$$

Then the DR resonance strength can expressed as

$$S_{ij}^{DR} = S_{ij}^{DC} B_j^r. \qquad (7)$$

In the isolated resonance approximation, assuming that the electron velocity distribution in the plasma is Maxwellian, the DR rate coeffcients can be expressed as

$$\alpha_i^{DR}(T_e) = \frac{h^3}{(2\pi m_e T_e)^{3/2}} \sum_j \frac{Q_j}{2g_i} \exp\left(-\frac{E_{ij}}{kT_e}\right), \qquad (8)$$

where Q_j is the so called intensity factor, defined as

$$Q_j = g_j A_{ji}^a B_j^r. \qquad (9)$$

The contributions from higher-n states are extrapolated up to $n = 1000$ using an empirical scaling formula (see Refs. [13, 14] for details).

In order to investigate the importance of DR on the plasma ionization balance, the corresponding three-body recombination (TR) and radiative recombination (RR) rate coefficients are also estimated by using formula given by Colombant and Tonon [17].

III. RESULTS AND DISCUSSION

In the present work, we report the results of detailed level-by-level calculations of the rate coefficients for DR through the following Pd-like gadolinium autoionizing inner-shell excited configuration complexes: $4d^9 4fnl$, $4p^5 4d^{10} 4fnl$, $4d^9 5l'nl$, $4d^9 6l'nl$ ($n \leqslant 18$, $l \leqslant 13$). These resonant configurations are associated with the $\Delta n = 0$, $\Delta n = 1$, and $\Delta n = 2$ core excitations, respectively. The configuration complexes used here are similar to those in Safronova and co-workers' work on Pd-like ions [13,14] except that we have explicitly included the contribution from states resulting from $4p$ excitation.

Energy levels, radiative transition probabilities, and autoionization rates of Ag-like gadolinium were calculated using the FAC code. The strongest lines with $Q_j > 5 \times 10^{12}$ s^{-1} for the $4d^9 4fnl$ and $4d^9 5l'nl$ complexes are presented in Tables I and II for RS and NRS decay, respectively. $4d^{10}nl$-$4d^9 4fnl$ transitions are nearly n independent as n increases, so only those states with $n \leqslant 7$ are shown for the $4d^9 4fnl$ complex.

It should be noted that not all the above listed doubly excited states can autoionize. Many of the configurations considered are below the first ionization limit as shown in Fig. 1.

A. DR through the $4d^9 4fnl$ complexes

The partial DR rate coefficient for production of $4d^9 4fnl$ complexes is presented in Fig. 2. It is shown that the relative contribution of these complexes to the total DR rate coefficient is greater than 69% at an electron temperature of around 110 eV; i.e., this complex gives the largest contribution to the total DR rate coefficient at 110 eV. For efficient EUV source operation this electron temperature is likely to be optimum in order to maximize conversion efficiency of input laser or discharge energy to EUV emission [18].

As one can see from Fig. 1, the doubly excited $4d^9 4f^2$, $4d^9 4f5l$ ($l \leqslant 3$), and $4d^9 4f6l$ ($l \leqslant 1$) configurations lie below the first ionization limit. Therefore, autoionizing intermediate states can be stabilized to these levels through nonresonant stabilizing transitions (NRS). Fow low-n' ($n' = 5$–7) states, the DR rate coefficient shows a rather complex dependence on temperature at values lower than 100 eV. This behavior

TABLE I. Resonant energies, Auger rates, radiative rates, intensity factors, and DR resonant strengths for RS decay for the $4d^9 4fnl$ and $4d^5 5l'nl$ levels. The states are denoted in jj coupling. A[B] denotes A $\times$ 10^{B}.

Low level	Upper level	E_{ij} (eV)	A^a (s^{-1})	$\sum A^r$ (10^{-12} s^{-1})	A^r (10^{-12} s^{-1})	Q_j (s^{-1})	S_{ij}^{DR} (10^{-18} eV cm^2)
$5g_{7/2}$	$(4d_{3/2}{}^5 4f_{7/2}5g_{7/2})_{9/2}$	7.229	1.880 [15]	5.404	4.277	4.265[13]	14.60
$5g_{9/2}$	$(4d_{3/2}{}^5 4f_{7/2}5g_{9/2})_{9/2}$	7.271	4.001 [14]	5.502	4.275	4.217[13]	14.36
$5g_{9/2}$	$(4d_{3/2}{}^5 4f_{7/2}5g_{9/2})_{11/2}$	7.311	2.304 [15]	5.425	4.652	5.569[13]	18.85
$5g_{9/2}$	$(4d_{3/2}{}^5 4f_{7/2}5g_{9/2})_{7/2}$	7.670	1.303 [14]	5.507	4.529	3.476[13]	11.22
$5g_{7/2}$	$(4d_{3/2}{}^5 4f_{7/2}5g_{7/2})_{5/2}$	7.675	1.303 [14]	5.504	4.687	2.698[13]	8.701
$6d_{3/2}$	$(4d_{3/2}{}^5 4f_{7/2}6d_{3/2})_{3/2}$	15.36	1.361 [13]	4.759	4.639	1.375 [13]	2.215
$6d_{3/2}$	$(4d_{3/2}{}^5 4f_{7/2}6d_{3/2})_{5/2}$	15.62	3.192 [14]	4.775	4.632	2.738 [13]	4.339
$6d_{3/2}$	$(4d_{3/2}{}^5 4f_{7/2}6d_{3/2})_{1/2}$	15.67	1.070 [14]	4.783	4.693	8.984[12]	1.419
$6d_{5/2}$	$(4d_{3/2}{}^5 4f_{7/2}6d_{5/2})_{5/2}$	16.33	4.390 [13]	4.760	4.617	2.499 [13]	3.787
$6d_{5/2}$	$(4d_{3/2}{}^5 4f_{7/2}6d_{5/2})_{7/2}$	16.59	3.483 [14]	4.778	4.688	3.700 [13]	5.518
$6d_{5/2}$	$(4d_{3/2}{}^5 4f_{7/2}6d_{5/2})_{3/2}$	16.62	1.776 [14]	4.780	4.661	1.815 [13]	2.703
$6f_{5/2}$	$(4d_{3/2}{}^5 4f_{7/2}6f_{5/2})_{7/2}$	43.00	1.527 [14]	4.653	4.548	3.530 [13]	2.032
$6f_{5/2}$	$(4d_{3/2}{}^5 4f_{7/2}6f_{5/2})_{5/2}$	43.03	1.564 [12]	4.562	4.476	6.858 [12]	0.395
$6f_{7/2}$	$(4d_{3/2}{}^5 4f_{7/2}6f_{7/2})_{7/2}$	43.20	8.870 [12]	4.567	4.549	2.402 [13]	1.376
$6f_{7/2}$	$(4d_{3/2}{}^5 4f_{7/2}6f_{7/2})_{9/2}$	43.24	1.769 [14]	4.642	4.552	4.435 [13]	2.539
$6f_{5/2}$	$(4d_{3/2}{}^5 4f_{7/2}6f_{5/2})_{3/2}$	43.27	1.530 [14]	4.581	4.572	1.776 [13]	1.016
$6f_{7/2}$	$(4d_{3/2}{}^5 4f_{7/2}6f_{7/2})_{5/2}$	43.46	1.655 [14]	4.582	4.493	2.623 [13]	1.494
$6g_{7/2}$	$(4d_{3/2}{}^5 4f_{7/2}6g_{7/2})_{9/2}$	6.193	1.193 [15]	5.251	4.565	4.545 [13]	1.816
$6g_{9/2}$	$(4d_{3/2}{}^5 4f_{7/2}6g_{9/2})_{9/2}$	6.196	1.096 [14]	5.339	4.564	4.352 [13]	1.738
$6g_{9/2}$	$(4d_{3/2}{}^5 4f_{7/2}6g_{9/2})_{11/2}$	6.198	1.321 [15]	5.273	4.661	5.571 [13]	2.225
$6g_{7/2}$	$(4d_{3/2}{}^5 4f_{7/2}6g_{7/2})_{5/2}$	62.16	1.157 [14]	5.326	4.679	2.684 [13]	1.069
$6g_{9/2}$	$(4d_{3/2}{}^5 4f_{7/2}6g_{9/2})_{7/2}$	62.17	1.155 [14]	5.327	4.535	3.468 [13]	1.381
$6h_{9/2}$	$(4d_{3/2}{}^5 4f_{7/2}6h_{9/2})_{11/2}$	65.66	3.688 [14]	4.667	4.580	5.427 [13]	2.046
$6h_{11/2}$	$(4d_{3/2}{}^5 4f_{7/2}6h_{11/2})_{13/2}$	65.67	3.693 [14]	4.667	4.667	6.452 [13]	2.432
$6h_{9/2}$	$(4d_{3/2}{}^5 4f_{7/2}6h_{9/2})_{7/2}$	65.71	1.552 [12]	4.671	4.671	9.319 [12]	0.351
$6h_{11/2}$	$(4d_{3/2}{}^5 4f_{7/2}6h_{11/2})_{9/2}$	65.72	1.524 [12]	4.671	4.592	1.130 [13]	0.426
$7s_{1/2}$	$(4d_{3/2}{}^5 4f_{7/2}7s_{1/2})_{3/2}$	45.17	3.126 [14]	4.889	4.674	1.841 [13]	1.009
$7s_{1/2}$	$(4d_{3/2}{}^5 4f_{7/2}7s_{1/2})_{1/2}$	45.17	2.350 [14]	4.889	4.674	9.157 [12]	0.502
$7p_{1/2}$	$(4d_{3/2}{}^5 4f_{7/2}7p_{1/2})_{1/2}$	52.89	1.001 [14]	4.897	4.793	9.139 [12]	0.428
$7p_{1/2}$	$(4d_{3/2}{}^5 4f_{7/2}7p_{1/2})_{3/2}$	52.91	3.363 [14]	4.918	4.806	1.895 [13]	0.886
$7p_{3/2}$	$(4d_{3/2}{}^5 4f_{7/2}7p_{3/2})_{3/2}$	55.45	5.522 [13]	4.869	4.800	1.764 [13]	0.788
$7p_{3/2}$	$(4d_{3/2}{}^5 4f_{7/2}7p_{3/2})_{5/2}$	55.56	3.299 [14]	4.890	4.810	2.844 [13]	0.127
$7p_{3/2}$	$(4d_{3/2}{}^5 4f_{7/2}7p_{3/2})_{1/2}$	55.65	1.336 [14]	4.881	4.803	9.266 [12]	0.412
$7d_{3/2}$	$(4d_{3/2}{}^5 4f_{7/2}7d_{3/2})_{3/2}$	68.42	9.053 [12]	4.706	4.640	1.221 [13]	0.442
$7d_{3/2}$	$(4d_{3/2}{}^5 4f_{7/2}7d_{3/2})_{5/2}$	68.55	1.787 [14]	4.713	4.635	2.710 [13]	0.978
$7d_{3/2}$	$(4d_{3/2}{}^5 4f_{7/2}7d_{3/2})_{1/2}$	68.59	7.622 [13]	4.718	4.681	8.817 [12]	0.318
$7d_{5/2}$	$(4d_{3/2}{}^5 4f_{7/2}7d_{5/2})_{5/2}$	68.97	2.264 [13]	4.715	4.627	2.298 [13]	0.825
$7d_{5/2}$	$(4d_{3/2}{}^5 4f_{7/2}7d_{5/2})_{7/2}$	69.11	1.914 [14]	4.723	4.679	3.653 [13]	1.308
$7d_{5/2}$	$(4d_{3/2}{}^5 4f_{7/2}7d_{5/2})_{3/2}$	69.13	1.184 [14]	4.726	4.652	1.789 [13]	6.406
$7f_{5/2}$	$(4d_{3/2}{}^5 4f_{7/2}7f_{5/2})_{5/2}$	84.35	1.136 [12]	4.559	4.471	5.351 [12]	0.157
$7f_{5/2}$	$(4d_{3/2}{}^5 4f_{7/2}7f_{5/2})_{7/2}$	84.36	7.608 [13]	4.619	4.527	3.415 [13]	1.002
$7f_{7/2}$	$(4d_{3/2}{}^5 4f_{7/2}7f_{7/2})_{7/2}$	84.46	5.619 [12]	4.564	4.527	1.998 [13]	0.587
$7f_{5/2}$	$(4d_{3/2}{}^5 4f_{7/2}7f_{5/2})_{3/2}$	84.49	1.080 [14]	4.570	4.556	1.748 [13]	0.512
$7f_{7/2}$	$(4d_{3/2}{}^5 4f_{7/2}7f_{7/2})_{9/2}$	84.49	8.886 [13]	4.613	4.546	4.321 [13]	1.266
$7f_{7/2}$	$(4d_{3/2}{}^5 4f_{7/2}7f_{7/2})_{5/2}$	84.61	1.156 [14]	4.571	4.481	2.586 [13]	0.757
$7g_{7/2}$	$(4d_{3/2}{}^5 4f_{7/2}7g_{7/2})_{9/2}$	95.55	7.055 [14]	5.050	4.541	4.508 [13]	1.168
$7g_{9/2}$	$(4d_{3/2}{}^5 4f_{7/2}7g_{9/2})_{9/2}$	95.58	7.450 [13]	5.109	4.540	4.249 [13]	1.100
$7g_{9/2}$	$(4d_{3/2}{}^5 4f_{7/2}7g_{9/2})_{11/2}$	95.58	7.918 [14]	5.062	4.666	5.564 [13]	1.441
$7g_{7/2}$	$(4d_{3/2}{}^5 4f_{7/2}7g_{7/2})_{5/2}$	95.69	8.710 [13]	5.102	4.676	2.650 [13]	0.686
$7g_{9/2}$	$(4d_{3/2}{}^5 4f_{7/2}7g_{9/2})_{7/2}$	95.70	8.685 [13]	5.102	4.544	3.433 [13]	0.888
$7h_{9/2}$	$(4d_{3/2}{}^5 4f_{7/2}7h_{9/2})_{11/2}$	98.10	3.345 [14]	4.664	4.574	5.413 [13]	1.366
$7h_{11/2}$	$(4d_{3/2}{}^5 4f_{7/2}7h_{11/2})_{13/2}$	98.11	3.352 [14]	4.664	4.664	6.439 [13]	1.625
$7h_{9/2}$	$(4d_{3/2}{}^5 4f_{7/2}7h_{9/2})_{7/2}$	98.14	1.914 [13]	4.666	4.666	1.086 [13]	0.274
$7h_{11/2}$	$(4d_{3/2}{}^5 4f_{7/2}7h_{11/2})_{9/2}$	98.14	1.879 [13]	4.666	4.585	1.317 [13]	0.332
$7i_{11/2}$	$(4d_{3/2}{}^5 4f_{7/2}7i_{11/2})_{13/2}$	98.37	4.854 [13]	4.669	4.607	5.884 [13]	1.480
$7i_{13/2}$	$(4d_{3/2}{}^5 4f_{7/2}7i_{13/2})_{15/2}$	98.37	4.850 [13]	4.669	4.669	6.815 [13]	1.715

TABLE I. (*Continued.*)

Low level	Upper level	E_{ij} (eV)	A^a (s^{-1})	$\sum A^r$ (10^{-12} s^{-1})	A^r (10^{-12} s^{-1})	Q_j (s^{-1})	S_{ij}^{DR} (10^{-18} eV cm^2)
$6g_{7/2}$	$(4d_{3/2}{}^5 5p_{3/2} 6g_{7/2})_{9/2}$	92.83	1.429 [13]	1.186	0.561	5.176 [12]	0.138
$6g_{9/2}$	$(4d_{3/2}{}^5 5p_{3/2} 6g_{9/2})_{11/2}$	92.85	2.152 [13]	1.198	0.574	6.527 [12]	0.174
$6h_{11/2}$	$(4d_{3/2}{}^5 5p_{3/2} 6h_{11/2})_{13/2}$	97.28	1.035 [13]	0.490	0.490	6.553 [12]	0.167
$7g_{9/2}$	$(4d_{3/2}{}^5 5p_{3/2} 7g_{9/2})_{11/2}$	126.8	1.086 [13]	0.941	0.551	6.080 [12]	0.119
$7h_{11/2}$	$(4d_{3/2}{}^5 5p_{3/2} 7h_{11/2})_{13/2}$	129.8	8.519 [12]	0.447	0.447	5.944 [12]	0.113
$7i_{13/2}$	$(4d_{3/2}{}^5 5p_{3/2} 7i_{13/2})_{15/2}$	130.2	1.544 [12]	0.412	0.412	5.203 [12]	0.099

occurs because the presence of some autoionizing levels very close to the ionization limit can considerably enhance the DR rate. Actually, in the present case, the $4d^9 4f5g$ configuration is the only intermediate state contributing to the DR rate coefficient as the other $5l$ states lie below the ionization limit as shown in Fig. 1. The $4d^9 4f5g$ configuration gives the biggest contribution in this complex for temperatures in the 3–20 eV region. This behavior has been observed in recent research on the contribution of near-threshold states to recombination [19]. In addition, the doubly excited $4d^9 4f$ $(6d,6f)$ and $4d^9 4f7s$ configurations are partially autoionizing as some of the levels have energies below the ionization limit. As a result, the contribution of these levels is also very important, as we can see from Eq. (3), since their resonant energies are quite small. The contribution of these low-n' states are highlighted in Fig. 3. The contributions from high-n' states are expected to be negligible for plasma temperatures below 50 eV. However, as the temperature increases, the contribution from high-n' states increases quickly and becomes nearly comparable to that from low-n' states above 100 eV.

TABLE II. Resonant energies, Auger rates, radiative rates, intensity factors, and DR resonant strengths for NRS decay for the $4d^9 4fnl$ and $4d^5 5l'nl$ levels. The states are denoted in jj coupling. A[B] denotes A $\times$ 10^B.

Low level	Upper level	E_{ij} (eV)	A^a (s^{-1})	$\sum A^r$ (10^{-12} s^{-1})	A^r (10^{-12} s^{-1})	Q_j (10^{-12} s^{-1})	S_{ij}^{DR} (10^{-18} eV cm^2)
$(4d_{3/2}{}^3 4f_{5/2}{}^2)_{7/2}$	$(4d_{5/2}{}^5 4f_{7/2} 5g_{7/2})_{9/2}$	7.229	1.880 [15]	5.404	0.553	5.509	1.886
$(4d_{3/2}{}^3 4f_{5/2} 4f_{7/2})_{7/2}$	$(4d_{5/2}{}^5 4f_{7/2} 5g_{9/2})_{9/2}$	7.271	4.001 [14]	5.502	0.684	6.746	2.296
$(4d_{3/2}{}^3 4f_{5/2} 4f_{7/2})_{9/2}$	$(4d_{5/2}{}^5 4f_{7/2} 5g_{9/2})_{11/2}$	7.311	2.304 [15]	5.425	0.732	8.768	2.968
$(4d_{3/2}{}^3 4f_{5/2} 4f_{7/2})_{5/2}$	$(4d_{5/2}{}^5 4f_{7/2} 5g_{9/2})_{7/2}$	7.670	1.303 [15]	5.507	0.692	5.308	1.713
$(4d_{3/2}{}^3 4f_{5/2} 4f_{7/2})_{7/2}$	$(4d_{5/2}{}^5 4f_{7/2} 6g_{9/2})_{9/2}$	61.96	1.096 [15]	5.339	0.575	5.482	0.219
$(4d_{3/2}{}^3 4f_{5/2} 4f_{7/2})_{9/2}$	$(4d_{5/2}{}^5 4f_{7/2} 6g_{9/2})_{11/2}$	61.98	1.321 [15]	5.273	0.562	6.719	0.268
$(4d_{5/2}{}^5 4f_{5/2} 5p_{1/2})_{11/2}$	$(4d_{5/2}{}^5 5p_{1/2} 5g_{7/2})_{13/2}$	25.16	1.598 [12]	1.005	0.829	7.123	0.701
$(4d_{3/2}{}^3 4f_{7/2} 5p_{1/2})_{9/2}$	$(4d_{3/2}{}^3 5p_{1/2} 5g_{9/2})_{11/2}$	32.85	3.148 [12]	1.051	0.751	6.755	0.509
$(4d_{3/2}{}^3 4f_{5/2} 5p_{1/2})_{7/2}$	$(4d_{3/2}{}^3 5p_{1/2} 5g_{7/2})_{9/2}$	33.62	1.805 [13]	1.149	0.607	5.710	0.420
$(4d_{3/2}{}^3 4f_{7/2} 5p_{3/2})_{13/2}$	$(4d_{3/2}{}^3 5p_{3/2} 5g_{9/2})_{15/2}$	42.92	1.570 [12]	1.003	0.951	9.290	0.536
$(4d_{3/2}{}^3 4f_{7/2} 5p_{3/2})_{9/2}$	$(4d_{3/2}{}^3 5p_{3/2} 5g_{9/2})_{11/2}$	43.12	5.075 [12]	1.088	0.751	7.418	0.426
$(4d_{5/2}{}^5 4f_{5/2} 5d_{5/2})_{15/2}$	$(4d_{5/2}{}^5 5d_{5/2} 5g_{7/2})_{17/2}$	87.93	6.789[11]	1.056	0.988	6.958	0.196
$(4d_{3/2}{}^3 4f_{5/2} 5d_{5/2})_{9/2}$	$(4d_{3/2}{}^3 5d_{5/2} 5g_{7/2})_{11/2}$	97.05	5.246 [12]	1.026	0.722	7.247	0.185
$(4d_{3/2}{}^3 4f_{5/2} 5d_{5/2})_{11/2}$	$(4d_{3/2}{}^3 5d_{5/2} 5g_{7/2})_{13/2}$	97.38	3.073 [12]	1.024	0.682	7.163	0.182
$(4d_{3/2}{}^3 4f_{5/2} 5d_{3/2})_{5/2}$	$(4d_{3/2}{}^3 5d_{3/2} 5g_{7/2})_{7/2}$	105.1	1.598 [14]	1.008	0.884	7.030	0.166
$(4d_{3/2}{}^3 4f_{7/2} 5d_{3/2})_{7/2}$	$(4d_{3/2}{}^3 5d_{3/2} 5g_{9/2})_{9/2}$	105.2	1.680 [14]	1.017	0.971	9.648	0.227
$(4d_{5/2}{}^5 4f_{7/2} 5f_{5/2})_{13/2}$	$(4d_{5/2}{}^5 5f_{7/2} 5g_{7/2})_{15/2}$	142.1	2.804 [12]	1.604	0.738	8.566	0.149
$(4d_{5/2}{}^5 4f_{7/2} 5f_{7/2})_{13/2}$	$(4d_{5/2}{}^5 5f_{7/2} 5g_{7/2})_{15/2}$	148.0	2.919 [12]	1.054	0.654	7.690	0.129
$(4d_{3/2}{}^3 4f_{7/2} 5f_{5/2})_{11/2}$	$(4d_{3/2}{}^3 5f_{7/2} 5g_{7/2})_{13/2}$	154.4	2.314 [12]	1.059	0.869	8.348	0.134
$(4d_{3/2}{}^3 4f_{7/2} 5f_{5/2})_{13/2}$	$(4d_{3/2}{}^3 5f_{7/2} 5g_{7/2})_{15/2}$	154.8	1.489 [12]	1.058	0.595	5.568	0.089
$(4d_{3/2}{}^3 4f_{5/2} 5f_{7/2})_{13/2}$	$(4d_{3/2}{}^3 5f_{7/2} 5g_{7/2})_{15/2}$	154.8	1.489 [12]	1.058	0.968	9.504	0.145
$(4d_{3/2}{}^3 4f_{7/2} 5s_{1/2})_{11/2}$	$(4d_{3/2}{}^3 5s_{1/2} 6g_{9/2})_{13/2}$	59.41	3.667 [12]	0.708	0.622	7.293	0.304
$(4d_{5/2}{}^5 4f_{5/2} 6s_{1/2})_{11/2}$	$(4d_{5/2}{}^5 5g_{7/2} 6s_{1/2})_{13/2}$	144.7	1.243 [12]	1.102	1.005	7.459	0.128
$(4d_{5/2}{}^5 4f_{5/2} 6s_{1/2})_{9/2}$	$(4d_{5/2}{}^5 5g_{7/2} 6s_{1/2})_{11/2}$	144.9	2.529 [12]	1.092	0.997	8.358	0.143
$(4d_{5/2}{}^5 4f_{7/2} 6s_{1/2})_{11/2}$	$(4d_{5/2}{}^5 5g_{9/2} 6s_{1/2})_{13/2}$	145.4	2.705 [12]	1.108	1.044	10.37	0.177
$(4d_{3/2}{}^3 4f_{7/2} 6s_{1/2})_{11/2}$	$(4d_{3/2}{}^3 5g_{9/2} 6s_{1/2})_{13/2}$	151.9	1.947 [12]	1.090	1.036	9.302	0.152
$(4d_{5/2}{}^5 4f_{7/2} 6p_{1/2})_{13/2}$	$(4d_{5/2}{}^5 5g_{9/2} 6p_{1/2})_{15/2}$	158.8	5.264[11]	1.119	1.109	5.678	0.089
$(4d_{3/2}{}^3 4f_{7/2} 6p_{1/2})_{9/2}$	$(4d_{3/2}{}^3 5g_{9/2} 6p_{1/2})_{11/2}$	165.9	1.178 [12]	1.177	0.877	5.267	0.786
$(4d_{3/2}{}^3 4f_{7/2} 6p_{1/2})_{9/2}$	$(4d_{3/2}{}^3 5g_{9/2} 6p_{1/2})_{11/2}$	167.0	1.396 [12]	1.145	0.865	5.703	0.846
$(4d_{3/2}{}^3 4f_{7/2} 6p_{3/2})_{3/2}$	$(4d_{3/2}{}^3 5g_{9/2} 6p_{3/2})_{15/2}$	170.9	5.728[11]	1.099	1.045	5.728	0.830
$(4d_{3/2}{}^3 4f_{7/2} 5d_{3/2})_{7/2}$	$(4d_{3/2}{}^3 5d_{3/2} 6g_{9/2})_{9/2}$	161.3	1.221 [14]	0.620	0.587	5.845	0.090

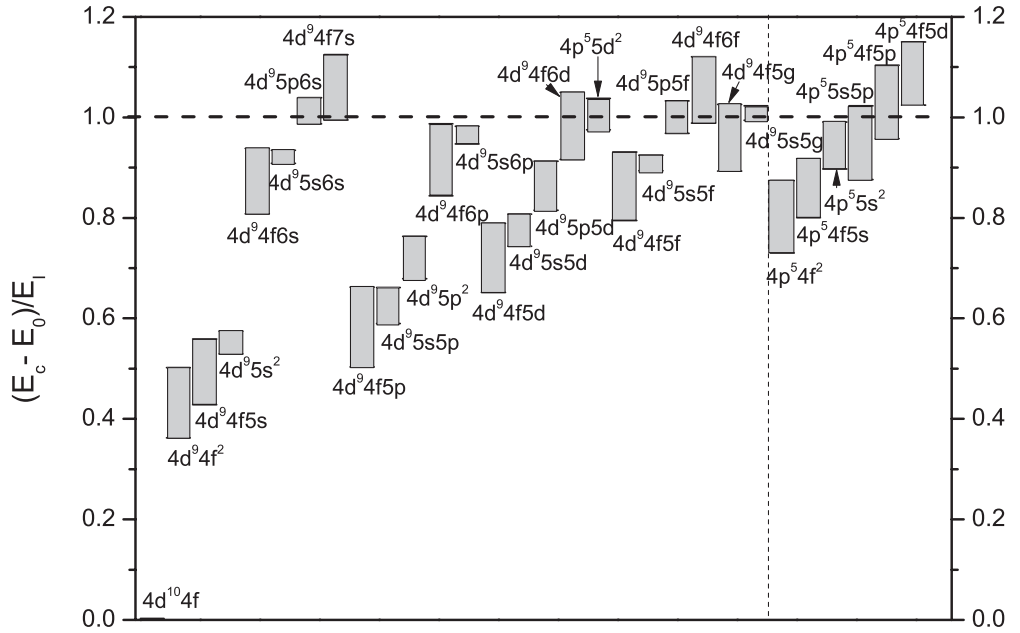

FIG. 1. Energy levels of doubly excited configurations within the $4d^94fnl$, $4d^95snl$, $4d^95pnl$, $4p^54d^{10}4fnl$, and $4p^54d^{10}5snl$ complex relative to the first ionization limit E_I (379.72 eV) which is indicated by the dashed line. E_0 is the ground state energy of Ag-like Gd. The energies are indicated by a finite vertical range representing the full level spread within each configuration.

B. DR through the $4p^54d^{10}4fnl$ complexes

The contributions from these complexes were ignored by Safronova *et al.* for Pd-like Xe and W [13,14]. However, as shown in Fig. 4 the calculations predict that the relative contribution of these complexes to the total DR rate coefficient is about 16% at an electron temperature close to 110 eV. In addition, we explored the influence of $4p^54d^{10}5l'nl$ and the results showed that their contributions are less than 3% of the total DR rate. The contribution from $4p^54d^{10}6l'nl$ complexes can be ignored in this temperature region. Consequently we just included their contribution in the total rate coefficients and do not discuss the details here.

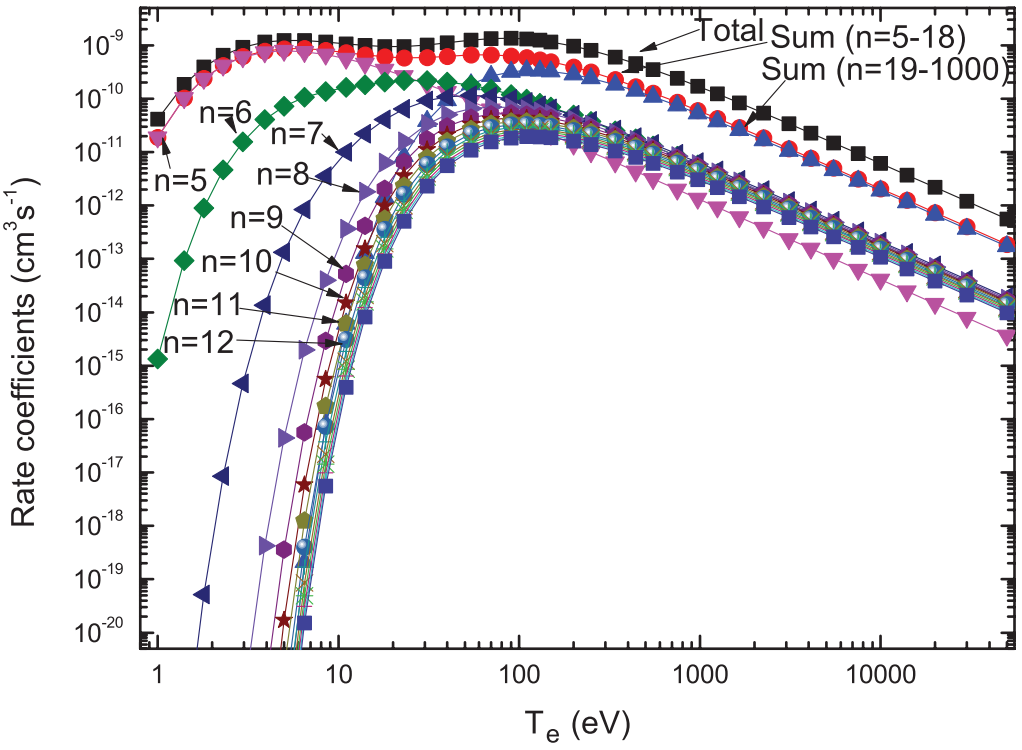

FIG. 2. (Color online) Partial DR rate coefficients for $4d^94fnl$ complexes.

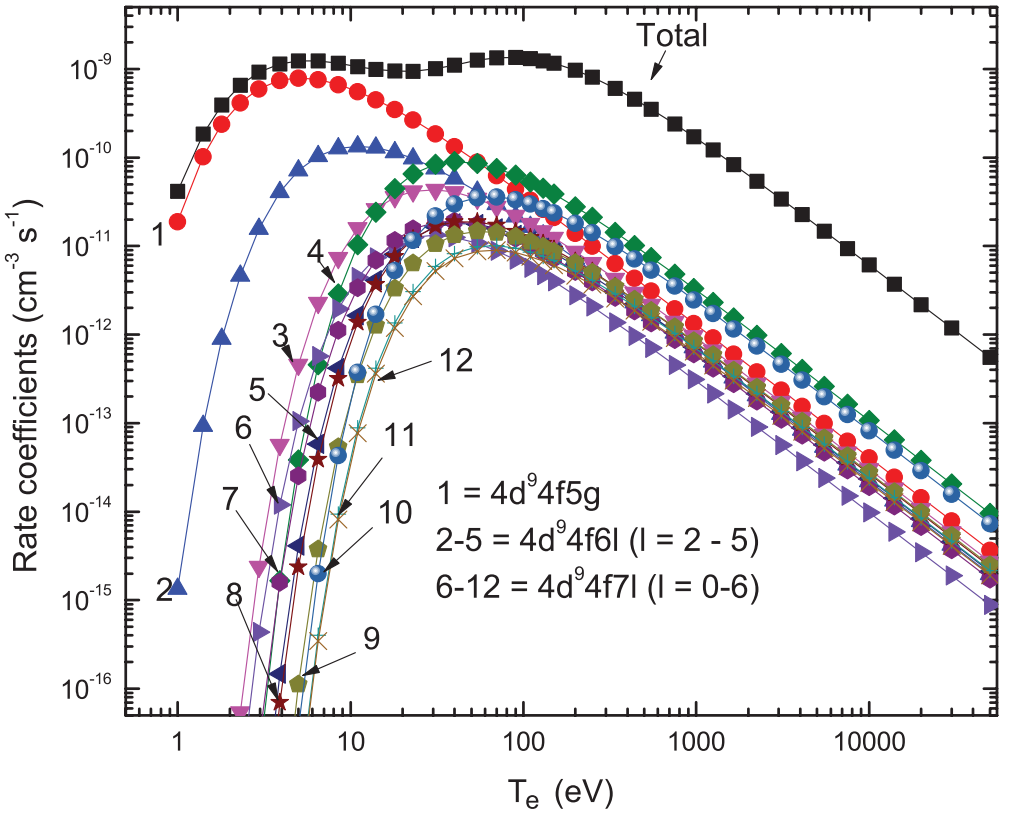

FIG. 3. (Color online) Contribution of low-n states to DR rate coefficients for the $4d^9 4fnl$ complexes.

Also from Fig. 1, we can see that the $4p^5 4d^{10} 4f^2$, $4p^5 4d^{10} 4f 5s$, and $4p^5 4d^{10} 5s^2$ are below the first ionization limit, so the autoionization channel is closed for these configurations. The $4p^5 4d^{10} 4f 5d$ configuration dominates in the 0–20 eV region and $4p^5 4d^{10} 4f 5f$ gives the main contribution in the 20–90 eV region. The reason is that many levels of the $4p^5 4d^{10} 4f 5p$ configuration lie below the ionization limit and so it is only partially autoionizing while

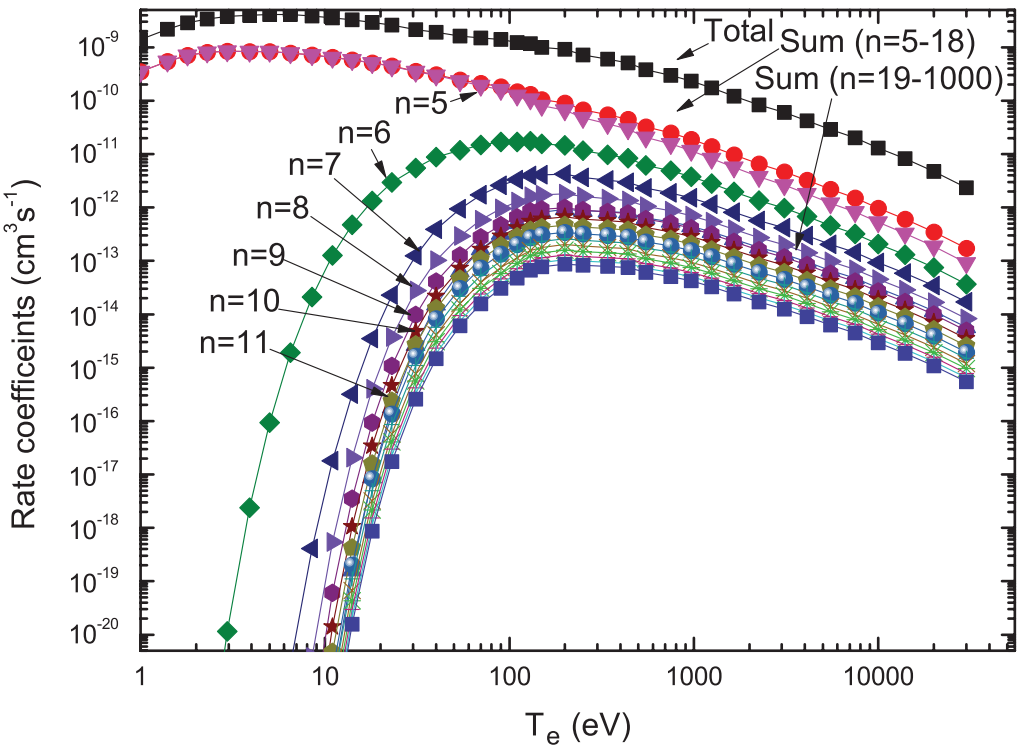

FIG. 4. (Color online) Partial DR rate coefficients for $4p^5 4d^{10}$ $4fnl$ complexes.

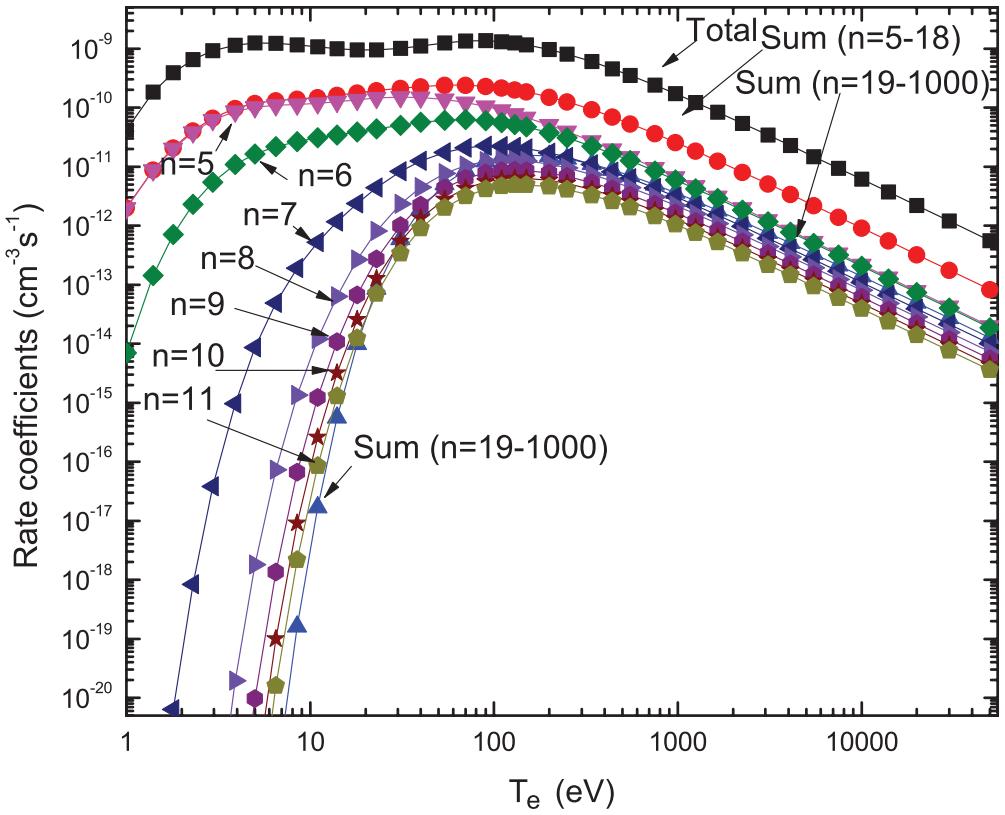

FIG. 5. (Color online) Partial DR rate coefficients for $4d^9 5l'nl$ complexes.

the $4p^5 4d^{10} 4f 5d$ configuration lies just above the ionization limit.

C. DR through the $4d^9 5l'nl$ complexes

The partial DR rate coefficients for $4d^9 5l'nl$ complexes are given in Fig. 5. The results show that these complexes contribute about 14% of the total DR rate coefficient at electron tempertures around 110 eV. That is to say this $\Delta n = 1$ core excitation is very important in the DR process. At temperatures below 100 eV, the $4d^9 5l'5l$ configuration gives the dominant contribution.

For this complex, the $4d^9 5s5l$ ($l \leqslant 3$) and $4d^9 5s6l$ ($l \leqslant 1$) configuratons lie below the first ionization limit. $4d^9 5p5f$ dominates when the electron temperature is less than 10 eV, and $4d^9 5d^2$ makes a sizable contribution in the 15–40 eV region. In addition, the $4d^9 5snl$ complexes have no autoionization channels, except for those connecting directly to the ground level of the Ag-like ion.

D. DR through the $4d^9 6l'nl$ complexes

The partial DR rate coefficients for $4d^9 6l'nl$ complexes are given in Fig. 6. All of these configurations lie entirely above the first ionization limit. The contribution from these complexes to the total DR rate coefficient is relatively small, about 0.09%, at an electron temperature around 110 eV. The dependence of partial DR rate coefficients on the temperature is quite regular for each of these configurations as all of their levels lie above the ionization limit.

In addition, it was found that contributions from $4s$ subshell excitations to the overall DR coefficient is less than 1.4% near 110 eV. Nevertheless, the partial rate coefficients for these are included in the total rate coefficients but we do not discuss them in more detail here.

E. The total DR rate coefficients

The resulting total DR rate coefficients are plotted together with RS and NRS transitions in Fig. 7. The NRS transitions are nearly comparable with RS around 100 eV. Contributions from $4s$ core excitation are too small and did not show in the figure. This predicts that we can ignore the effects of $4s$ core excitation for Ag-like and Rh-like Gd. For $4p$ core excitation, direct calculation for $n = 8$ should be sufficient; higher-n contributions can be calculated by the scaling formula [13,14].

F. Influence of DR processes on ionization balance in plasma

The behavior of the main recombination rate coefficients as a function of temperature is shown in Fig. 8. The TR rate coefficients were calculated for two electron densities, $n_{e1} = 10^{20}$ cm^{-3} and $n_{e2} = 10^{19}$ cm^{-3}, respectively, which are typical of electron densities encountered in laser produced plasma (LPP) and discharge produced plasma (DPP) extreme ultraviolet lithography (EUVL) sources. It is clear that the rate coefficient for DR is almost one order of magnitude greater than the rate coefficients for either of the other two

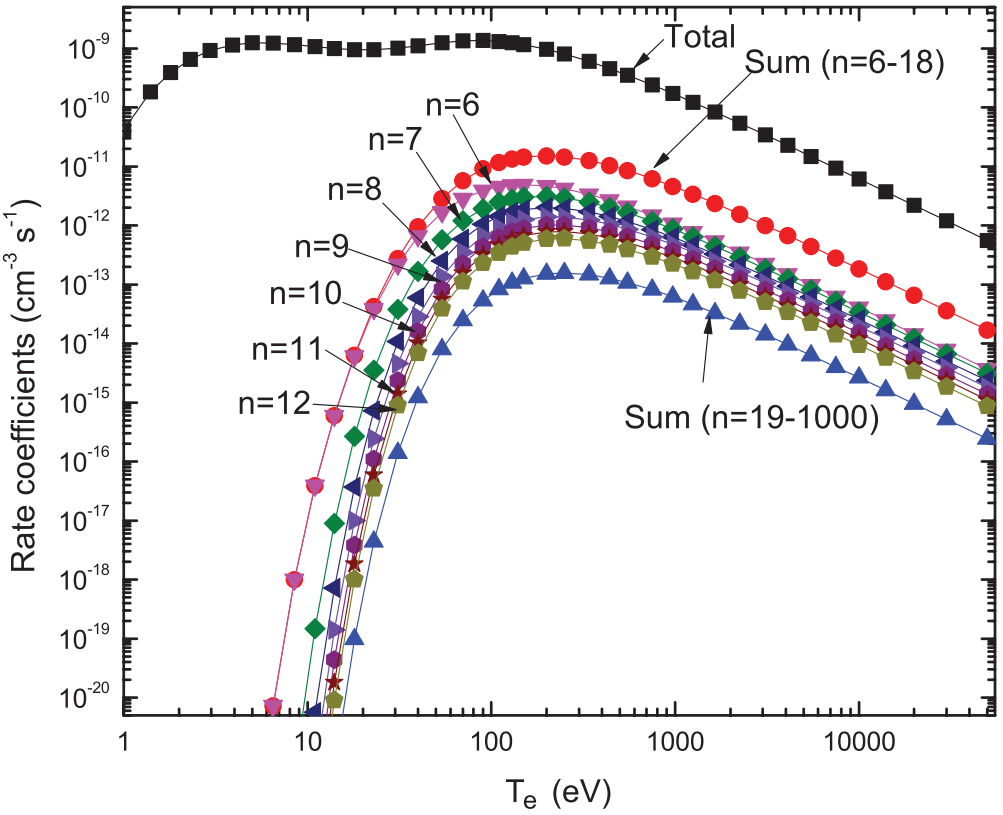

FIG. 6. (Color online) Partial DR rate coefficients for $4d^9 6l'nl$ complexes.

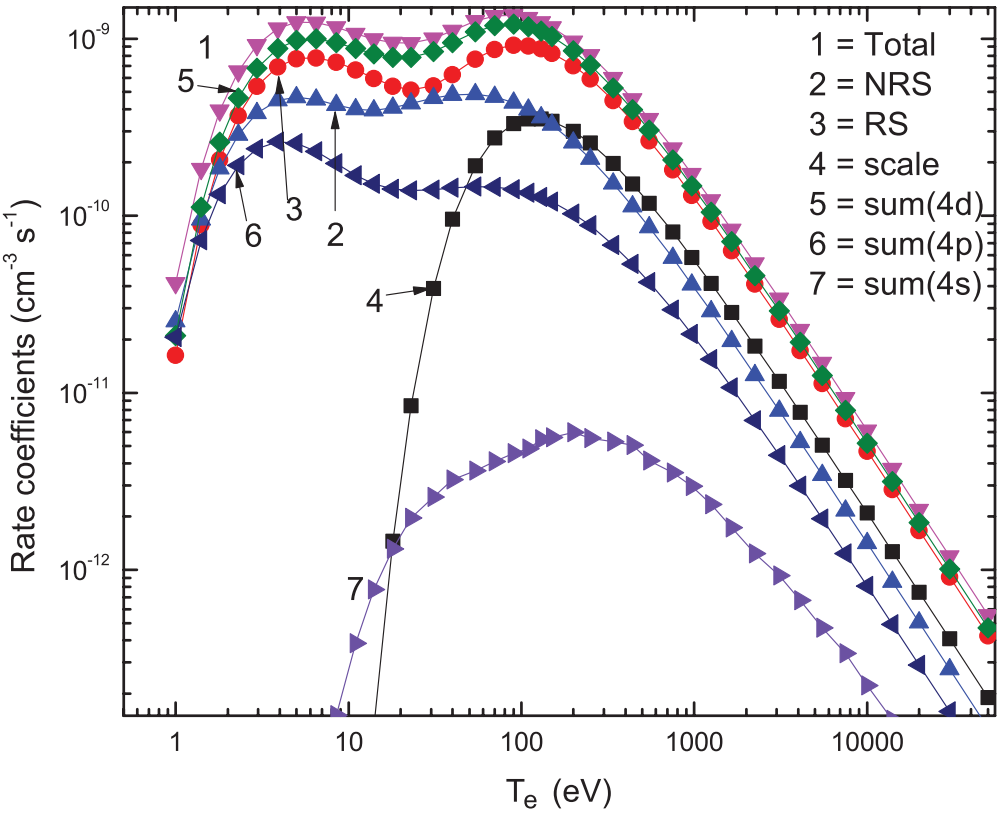

FIG. 7. (Color online) Contributions from the RS and NRS transition as well as different core excitations to total DR rate coefficients as a function of T_e in Pd-like Gd.

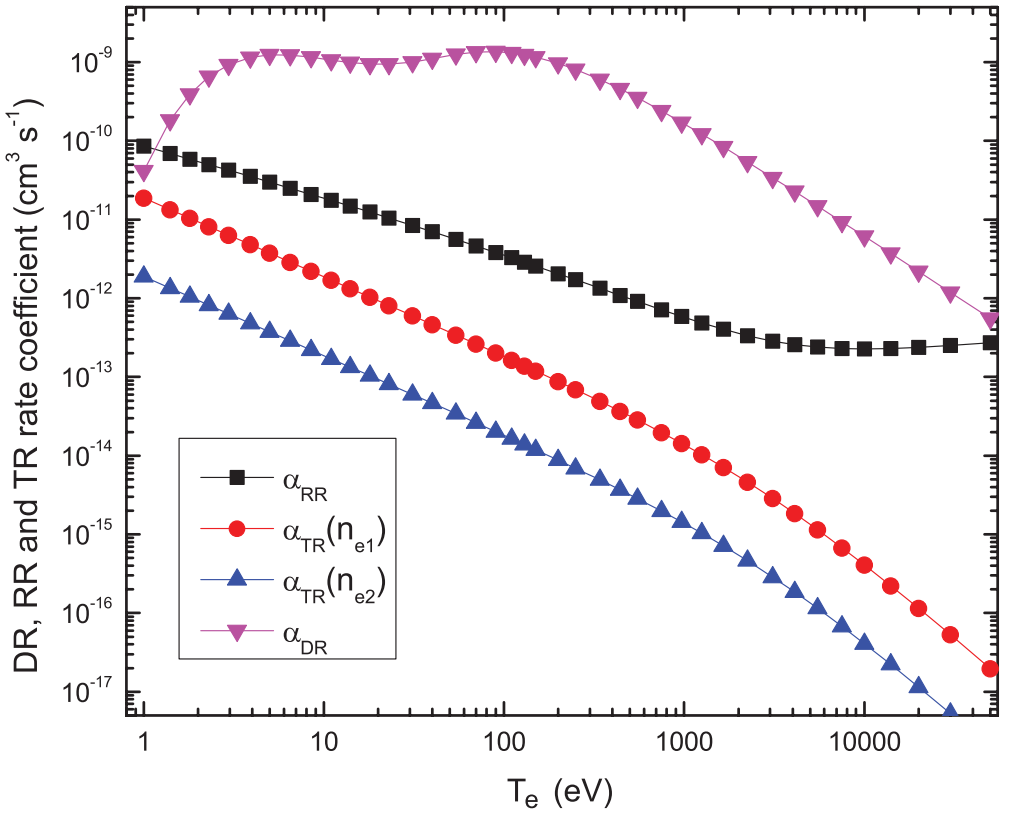

FIG. 8. (Color online) Comparison of the DR, TR, and RR rate coefficients for Pd-like Gd. The TR rate coefficients calculated for two electron densities, $n_{e1} = 10^{20}$ cm^{-3} and $n_{e2} = 10^{19}$ cm^{-3}, are presented.

recombination processes, RR and TR, near 110 eV. These results imply that DR will change the plasma ionization balance significantly. However, the DR process has been ignored in many collisional-radiative (CR) models either because of the complexity involved in calculating reliable data or because it was assumed that DR did not make a dramatic contribution in such plasmas. When considering relative ion abundances in Gd plasmas, the omission of DR will result in an underestimate of the plasma temperature.

IV. CONCLUSION

In this paper, detailed calculations of the DR rate coefficients for Pd-like Gd have been presented. The total DR rate coefficient was compared with the three-body and radiative recombination rate coefficients and it was found that the DR process is the dominant recombination mechanism in Pd-like gadolinium and will influence the ionization balance in a Gd plasma. The rate coefficients calculated in the present work will be useful for modeling spectral emission in hot plasmas for EUV source development. DR rate coefficients for Ag-like and Rh-like gadolinium ions will be studied in a future work.

ACKNOWLEDGMENTS

We would like to acknowledge support from Science Foundation Ireland under Grant No. 07/IN.1/I1771. One of the authors (B.L.) would like to acknowledge financial support from a UCD-CSC scholarship award.

[1] G. Tallents, E. Wagenaars, and G. Pert, Nat. Photonics **4**, 809 (2010).
[2] V. Y. Banine, K. N. Koshelev, and G. H. P. M. Swinkels, J. Phys. D **44**, 253001 (2011).
[3] W. Svendsen and G. O'Sullivan, Phys. Rev. A **50**, 3710 (1994).
[4] S. S. Churilov and A. N. Ryabtsev, Phys. Scr. **73**, 614 (2006).
[5] G. O'Sullivan and R. Faulkner, Opt. Eng. **33**, 3978 (1994).
[6] S. S. Churilov, R. R. Kildiyarova, A. N. Ryabtsev, and S. V. Sadovsky, Phys. Scr. **80**, 045303 (2009).
[7] D. Kilbane and G. O'Sullivan, J. Appl. Phys. **108**, 104905 (2010).
[8] T. Higashiguchi, T. Otsuka, N. Yugami, W. H. Jiang, A. Endo, B. W. Li, D. Kilbane, P. Dunne, and G. O'Sullivan, Appl. Phys. Lett. **99**, 191502 (2011).
[9] Y. B. Fu, C. Z. Dong, M. G. Su, and G. O'Sullivan, Chin. Phys. Lett. **25**, 972 (2008).
[10] Y. B. Fu, C. Z. Dong, M. G. Su, F. Koike, G. O'Sullivan, and J. G. Wang, Phys. Rev. A **83**, 062708 (2011).
[11] J. Sugar, V. Kaufman, and W. L. Rowan, J. Opt. Soc. Am. B **10**, 1321 (1993).
[12] J. Sugar, V. Kaufman, and W. L. Rowan, J. Opt. Soc. Am. B **10**, 799 (1993).

[13] U. I. Safronova, R. Bista, R. Bruch, and Yu. Ralchenko, J. Phys. B **42**, 015001 (2009).
[14] U. I. Safronova, A. S. Safronova, P. Beiersdorfer, and W. R. Johnson, J. Phys. B **44**, 035005 (2011).
[15] M. F. Gu, Astrophys. J. **590**, 1131 (2003).
[16] E. Behar, P. Mandelbaum, J. L. Schwob, A. Bar-Shalom, J. Oreg, and W. H. Goldstein, Phys. Rev. A **52**, 3770 (1995).
[17] D. G. Colombant and D. F. Tonon, J. Appl. Phys. **44**, 3524 (1973).
[18] B. W. Li, P. Dunne, T. Higashiguchi, T. Otsuka, N. Yugami, W. H. Jiang, A. Endo, and G. O'Sullivan, Appl. Phys. Lett. **99**, 231502 (2011).
[19] F. Robicheaux, S. D. Loch, M. S. Pindzola, and C. P. Ballance, Phys. Rev. Lett. **105**, 233201 (2010).